ACS OMEGA

http://pubs.acs.org/journal/acsodf

Article

Diffusion of Squalene in Nonaqueous Solvents

Bruce A. Kowert*

Cite This: *ACS Omega* 2022, 7, 31424−31430

Read Online

ACCESS | Metrics & More | Article Recommendations

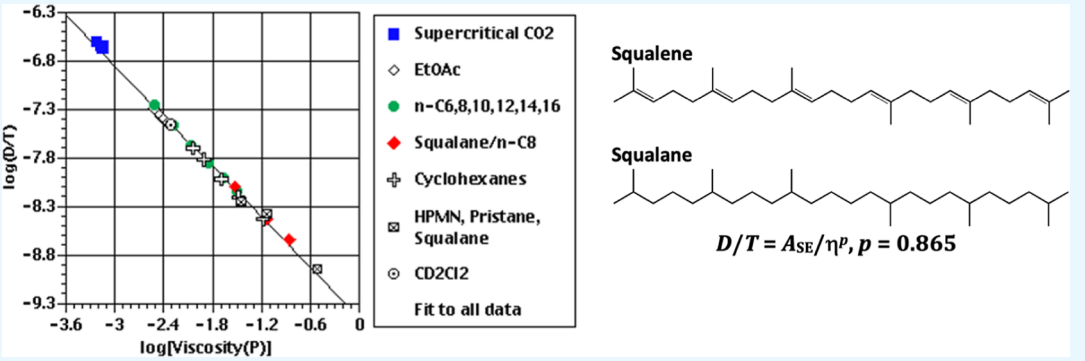

ABSTRACT: Capillary flow techniques have been used to determine the translational diffusion constant, D, of squalene in seven alkanes and five cyclohexanes. The alkanes are *n*-hexane, *n*-octane, *n*-decane, *n*-dodecane, *n*-tetradecane, 2,2,4,4,6,8,8-heptamethylnonane (isocetane), and 2,6,10,14-tetramethylpentadecane (pristane). The cyclohexanes are cyclohexane, *n*-butylcyclohexane, *n*-hexylcyclohexane, *n*-octylcyclohexane, and *n*-dodecylcyclohexane. When combined with published data in CD_2Cl_2, ethyl acetate, *n*-hexadecane, squalane, *n*-octane−squalane mixtures, and supercritical CO_2, the 35 diffusion constants and viscosities, η, vary by factors of ∼230 and ∼500, respectively. A fit to the modified Stokes−Einstein equation (MSE, $D/T = A_{SE}/\eta^p$) gives an average absolute percentage difference (AAPD) of 7.72% between the experimental and calculated D values where p and A_{SE} are constants, T is the absolute temperature, and the AAPD is the average value of (10^2) $(|D_{calcd} - D_{exptl}|/D_{exptl})$. Two other MSE fits using subsets of the 35 diffusion constants may be useful for (a) estimating the viscosity of the hydrophobic core of lipid droplets, where squalene is a naturally occurring component, and (b) providing estimates of the D values needed to design extraction processes by which squalene is obtained from plant oils. The Wilke−Chang equation also was considered and found to give larger AAPDs than the corresponding MSE fits.

INTRODUCTION

Squalene is a triterpene with a 24-carbon backbone, six methyl groups, and six isolated double bonds (Figure 1). In addition to its antioxidant and anti-inflammatory properties,[1] it is one of the major lipids on the surface of human skin and its reaction with ozone has been studied because of the role it plays in indoor air quality.[2] An intermediate in the biosynthesis of cholesterol,[1] squalene is found in the hydrophobic core of lipid droplets.[3,4] In ref 5, we suggested that if its translational diffusion constant, D, was measured in a lipid droplet, our D values in five alkanes could be used to make a label-free estimate of the droplet's viscosity, η. This was worth pursuing because lipid droplet viscosities depend on the cell type; the D values of the probe coumarin 153 (C153) indicated that the droplets of a human lung cancer cell were 66% more viscous than those in a non-cancer lung fibroblast cell.[6]

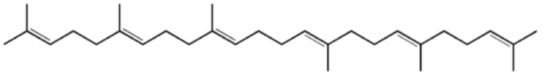

Figure 1. Structure of squalene.

Lipid droplet viscosities also can differ from those of other cell components. C153 showed that the droplets of a Chinese hamster ovary cell[7] were ∼2.4 times more viscous than its nucleus and cytoplasm. Additionally, viscosity would show how readily triacylglycerides and sterol esters move through a droplet to its surface, where they participate in the reactions that play a primary role in intercellular defense.[8,9] Measuring the viscosity as a function of temperature could give information about phase transitions such as the liquid−liquid crystal transition that has

Received: June 20, 2022
Accepted: August 5, 2022
Published: August 23, 2022

Table 1. Squalene Diffusion Constants

solvent	T, °C	10^6D, cm^2/s	$10^2\eta$, P[a]	r, Å[b]	% difference no CO_2[c]	% difference no HPSM[d]	% difference all 35[e]
n-C_6	23.0	16.50	0.306	4.30	−11.2	−4.51	−4.51
n-C_8	24.0	10.07	0.514	4.20	−4.99	−1.88	0.17
n-C_{10}	24.0	6.27	0.850	4.08	0.70	−0.006	4.15
n-C_{12}	24.0	4.18	1.41	3.70	−0.52	−5.01	0.95
n-C_{14}	24.0	2.91	2.14	3.50	1.28	−6.38	1.15
n-C_{16}[f]	22.75	2.10	3.18	3.24	0.38	−10.0	−1.26
$x_i = 0.291$[f]	22.5	2.36	2.97	3.08	−5.62	−15.0	−6.92
$x_i = 0.508$[f]	22.75	1.11	7.24	2.69	−3.77	−19.1	−8.25
$x_i = 0.708$[f]	22.5	0.670	13.8	2.35	−6.28	−25.1	−12.8
squalane[f]	23.0	0.336	30.3	2.13	−2.39	−26.6	−11.8
pristane	22.25	1.25	7.28	2.38	−14.9	−28.5	−18.8
HPMN	24.0	1.64	3.52	3.71	17.0	4.07	14.7
cyclohexane	24.0	5.88	0.910	4.06	1.39	0.15	4.59
n-$C_4C_6H_{11}$	24.0	4.48	1.23	3.96	4.09	−7.77	6.17
n-$C_6C_6H_{11}$	24.5	2.85	2.02	3.79	8.50	0.74	8.60
n-$C_8C_6H_{11}$	23.25	1.84	3.24	3.64	13.3	1.36	11.4
n-$C_{12}C_6H_{11}$	24.0	1.10	6.53	3.04	6.71	−9.51	2.21
CD_2Cl_2[g]	10.0	9.82	0.482	4.38	−2.10	1.61	3.46
CO_2, 18 MPa[h]	41.35	68	0.0728	4.65	−25.0	−9.83	−14.8
CO_2, 17 MPa	41.35	71	0.0709	4.58	−26.6	−11.5	−16.5
CO_2, 16 MPa	41.35	66	0.0688	5.07	−19.0	−2.24	−7.87
CO_2, 15 MPa	41.35	71	0.0665	4.88	−22.5	−6.24	−11.8
CO_2, 13 MPa	41.35	78	0.0602	4.91	−23.5	−6.59	−12.4
EtOAc, 1 bar[i]	30.0	11.71	0.399	4.75	2.78	8.26	9.41
EtOAc, 75 bar	30.0	10.98	0.433	4.67	2.45	7.22	8.72
EtOAc, 150 bar	30.0	10.52	0.464	4.55	1.00	5.13	6.89
EtOAc, 1 bar	40.0	13.38	0.359	4.77	1.41	7.69	8.39
EtOAc, 75 bar	40.0	12.65	0.390	4.65	0.16	5.68	6.70
EtOAc, 150 bar	40.0	11.88	0.419	4.61	0.51	5.46	6.79
EtOAc, 1 bar	50.0	15.14	0.325	4.81	0.42	7.46	7.72
EtOAc, 75 bar	50.0	14.19	0.354	4.71	−0.17	6.12	6.75
EtOAc, 150 bar	50.0	13.38	0.381	4.64	−0.37	5.31	6.24
EtOAc, 1 bar	60.0	17.22	0.295	4.80	−1.38	6.34	6.18
EtOAc, 75 bar	60.0	16.03	0.323	4.71	−1.72	5.23	5.46
EtOAc, 150 bar	60.0	15.00	0.348	4.67	−1.25	5.11	5.65

[a]From the refs in the Experimental Methods section. [b]Calculated from the D values using eq 1. [c]Percentage differences between 30 calculated and experimental D values using fit to eq 2 excluding CO_2 data. [d]Same as footnote *c* using fit to eq 2 for 29 D values excluding HPSM data. [e]Same as footnote *c* using fit to eq 2 for all 35 experimental D values. [f]From ref 5 (x_i = mole fraction squalane in *n*-C_8−squalane mixed solvents). [g]From ref 12. [h]All CO_2 D values are from ref 14. [i]All EtOAc D values are from ref 13.

been observed in the lipid droplets of cultured Huh7 cells.[10] These transitions have been studied in low-density lipoproteins as a function of composition and pressure and are reviewed in ref 11. The transitions have not been studied to the same degree in lipid droplets and new results could help elucidate their role in biological functions.

Estimates of lipid droplets' viscosities should be made using the widest possible range of diffusion constants and viscosities but the values in ref 5 varied by factors of only ∼7 and ∼10, respectively. Their ranges have been expanded in this paper. The diffusion constants for squalene in seven alkanes and five cyclohexanes have been determined using capillary flow techniques. The alkanes are *n*-hexane, *n*-octane, *n*-decane, *n*-dodecane, *n*-tetradecane, 2,2,4,4,6,8,8-heptamethylnonane (HPMN), and 2,6,10,14-tetramethylpentadecane (pristane). The cyclohexanes are cyclohexane, *n*-butylcyclohexane, *n*-hexylcyclohexane, *n*-octylcyclohexane, and *n*-dodecylcyclohexane. When combined with squalene's diffusion constants in *n*-hexadecane,[5] squalane,[5] *n*-octane-squalane mixtures,[5] CD_2Cl_2,[12] compressed ethyl acetate (EtOAc),[13] and supercritical CO_2,[14] the 35 values of D and η vary by factors of ∼230 and ∼500, respectively (Table 1). A fit to the modified Stokes−Einstein equation (MSE)[5] gave an average absolute percentage difference (AAPD) of 7.72% between the experimental and calculated D values, less than that of the Wilke−Chang equation[15] (11.2%), an oft-employed correlation in analytical chemistry. The AAPD is the average value of (10^2) ($|D_{calcd} - D_{exptl}|/D_{exptl}$).

Two other MSE fits have been made that may be useful for estimating the viscosities of lipid droplets and the diffusion constants needed to design the supercritical and pressurized extractions by which squalene can be obtained from plant sources.[13] These separations have become more important because international regulations reduced the supply of squalene's traditional source, shark liver oil.[1,13] Our diffusion constants for squalene also may be useful for checking molecular dynamics (MD) computer codes[16,17] and machine learning (ML) diffusion constant predictions.[18,19]

https://doi.org/10.1021/acsomega.2c03842
ACS Omega 2022, 7, 31424−31430

EXPERIMENTAL METHODS

Chemicals and Sample Preparation. In this and the following sections, n-C_i is used for the n-alkanes and n-$C_iC_6H_{11}$ is used for the cyclohexanes. Chemicals were obtained and used as received from (a) Sigma-Aldrich: pristane (98%), n-C_6 (≥99%), and n-C_{10} (99+%); (b) Aldrich: HPMN (98%), n-C_8 (99+%), n-C_{14} (99+%), and n-$C_4C_6H_{11}$ (99+%); (c) Sigma: squalene (≥98%) and n-C_{12} (99%); (d) Fisher: cyclohexane (99.9%); and (e) TCI: n-$C_6C_6H_{11}$ (>98.0%), n-$C_8C_6H_{11}$ (>98.0%), and n-$C_{12}C_6H_{11}$ (>98.0%). Squalene was stored in a cooler at 4 °C. Samples were prepared and profiles were taken with the laboratory lights off to minimize the possibility of photo-oxidation.[20]

Profile Acquisition and Analysis. The sigmoidal elution profiles used to determine squalene's D values were obtained[5,21] using a Thermo Separation Products SC100 variable wavelength detector, Chrom Perfect software (Justice Innovations), and a fused silica microcapillary (Polymicro Technology, 76.5 μm i.d). The detector wavelength was 198 nm.[20] Profiles were taken at room temperature (Table 1), which varied by no more than ±0.25 °C during a given acquisition. The experimental profiles were compared with those calculated using Taylor's equations.[5,22−25] The D values, with uncertainties of ±5%, are given in Table 1, along with the average values in squalane,[5] n-C_{16},[5] the n-C_8−squalane mixtures,[5] CD_2Cl_2,[12] EtOAc,[13] and supercritical CO_2.[14]

Solvent Viscosities. The viscosities for squalene's solvents are given in Table 1. Those for n-C_i (i = 6, 8,10, 12, 14, and 16) are from ref 26. Those for HPMN, pristane, and squalane are from refs 27, 28, and 29, respectively. The viscosities for the other solvents were determined by interpolation from the following sources: cyclohexane, ref 30; n-$C_4C_6H_{11}$, n-$C_6C_6H_{11}$, n-$C_8C_6H_{11}$, and n-$C_{12}C_6H_{11}$, ref 31; supercritical CO_2, ref 32; and CD_2Cl_2, ref 33. The viscosities for the n-C_8−squalane mixed solvents with squalane mole fractions x_i = 0.291, 0.508, and 0.708 are from ref 5. Those for EtOAc are from ref 13.

RESULTS

Viscosity and Temperature Dependence of D Values. The analysis of squalene's diffusion constants starts with the Stokes−Einstein relation[34,35]

$$D = k_B T/(6\pi\eta r) \quad (1)$$

where k_B is Boltzmann's constant, T is the absolute temperature, and r is the solute's hydrodynamic radius. The Stokes−Einstein limit, which would give a common r value for a given solute in a series of solvents, requires the solute to be much larger than the solvent.[35] Squalene is not in this limit; its r values in the n-alkanes, cyclohexanes, n-C_8−squalane mixed solvents, and methyl-substituted alkanes (HPMN, pristane, and squalane) decrease as the viscosity increases (Table 1). This dependence of a solute's size parameter on viscosity[21,36] has been attributed to solute−solvent interactions.[37] A larger value indicates stronger coupling of the solute's motion to the solvent's flow.[37]

When r decreases as η increases, following the early work of Chen, Davis, and Evans,[38] we[5,21,36] and others[39,40] have fitted the D values for a given solute in a series of solvents to the MSE[5,38]

$$D/T = A_{SE}/\eta^p \quad (2)$$

where p and A_{SE} are constants and p = 1 for the Stokes−Einstein limit. The p values for 26 hydrocarbons in n-alkanes and squalane[21] showed the expected increase in p as the solute size increased. Representative values[21] ranged from 0.656 ± 0.017 for 1-hexene to 0.953 ± 0.020 for rubrene.

Squalene's D values were used for three fits to eq 2. All had ranges of viscosity and diffusion constants larger than those in ref 5. The values of p, A_{SE}, and R^2 for the fits are given in Table 2.

Table 2. Values of p, −Log A_{SE}, and R^2 for the Fits of Squalene's D Values to eq 2

solvents	P	−log A_{SE}	R^2
all 35[a]	0.865 ± 0.007	9.449 ± 0.017	0.995
no CO_2[b]	0.827 ± 0.009	9.385 ± 0.021	0.997
no HPSMs[c]	0.905 ± 0.008	9.549 ± 0.018	0.997

[a]All 35 of the D values in Table 1 are included. [b]The five D values in CO_2 are excluded. [c]The six D values in the HPSMs are excluded.

The differences between the experimental D values and the values calculated for each solvent for each fit are given in Table 1. The AAPD by the solvent group and the total AAPD for each fit are given in Table 3.

Table 3. AAPD between Experimental and Calculated Diffusion Constants for the Three Fits to eq 2

solvent type	no. of solvents	no CO_2[a]	no HPSMs[a]	all[a]
HPSM	6	8.33	19.7	12.2
CO_2	5	23.3	7.28	12.7
n-C_i	6	3.18	4.63	2.03
cyclohexanes	5	6.80	3.91	6.59
CD_2Cl_2	1	2.10	1.61	3.46
EtOAc	12	1.13_5	6.25	7.07_5
AAPD for included		3.96[b]	5.53[c]	7.72[d]

[a]AAPD between experimental and calculated D values for each solvent group. [b]AAPD for 30 solvents excluding CO_2 data. [c]AAPD for 29 solvents excluding HPSM data. [d]AAPD for all 35 solvents.

The first fit, shown in Figure 2, used all 35 of the diffusion constants and gave an AAPD of 7.72%. This is reasonably good

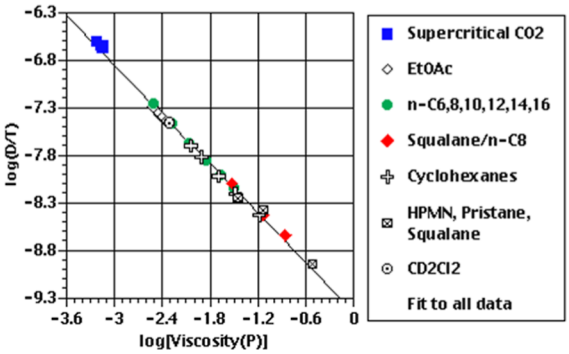

Figure 2. Plot of $\log(D/T)$ vs. $\log\eta$ for squalene. D is in $cm^2\ s^{-1}$ and η in P. The line is drawn using the fit to eq 2 for all 35 of squalene's D values.

agreement for D values and viscosities that vary by factors of ~230 and ~500, respectively, in solvents with different shapes, sizes, and structures. The fit (Table 3) gave an AAPD of 12.7% for the least viscous CO_2 solutions and 12.2% for the most viscous group, the HPSMs (HPMN, pristane, squalane, and the n-C_8−squalane mixtures). The largest AAPD of the other groups was 7.07_5% for the EtOAc solutions. Nine of the individual

https://doi.org/10.1021/acsomega.2c03842
ACS Omega 2022, 7, 31424−31430

differences (Table 1) had absolute differences greater than 10%, the largest was −18.8% in pristane. The values of D calculated from this fit are plotted against the experimental values as shown in Figure 3.

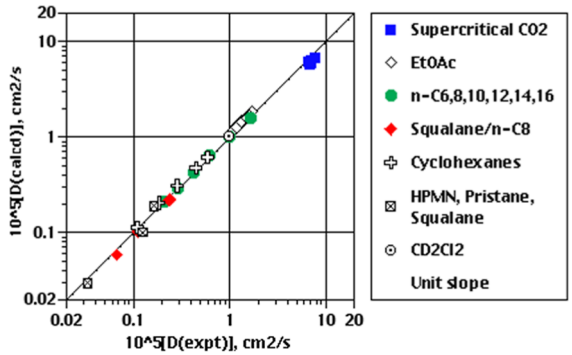

Figure 3. Plot of calculated *vs.* experimental diffusion constants for squalene. The calculated values were obtained using the MSE fit to eq 2 for all 35 of squalene's D values.

The other two fits focused on the high and low ends of the viscosity range. The CO_2 viscosities are clearly the lowest of those given in Table 1. The other 30 solutions have values of D and η that vary by factors of ∼50 and ∼100, respectively, and their fit to eq 2 gave an AAPD of only 3.96% (Table 3). The AAPD for the HPSMs, 8.33%, was smaller than that for the all-inclusive fit and that for the excluded CO_2 diffusion constants was predictably higher, 23.3%. The absolute differences for only four of the 30 D values used in the fit were >10% (Table 1). The largest was +17.0% for HPMN.

The third fit omitted the D values for the six HPSMs and improved the agreement for the low viscosity CO_2 solutions. Their AAPD, 7.28%, was smaller than that for the 35-solution fit, 12.7% (Table 3). The AAPD for the 29 solutions used in the fit (5.53%) also was relatively small. Their diffusion constants and viscosities varied by factors of ∼70 and ∼110, respectively (Table 1). The largest AAPD of the other groups was 6.25% for EtOAc. Except for the excluded HPSMs (AAPD of 19.7%, Table 3), only CO_2 at 17 MPa (−11.5%) and n-C_{16} (−10.0%) had absolute differences ≥10% (Table 1). The agreement for the D values in CO_2 is probably the best that can be expected, given that they were taken at the same temperature with small differences in the supercritical pressure and do not follow the viscosities (Table 1).

DISCUSSION

Lipid Droplets. In ref 5, we noted that a viscosity close to that of squalane had been reported in a lipid droplet.[7] Bhattacharyya and co-workers used fluorescence correlation spectroscopy and C153 to determine η = 34 cP at 25 °C in the droplet of a live Chinese hamster ovary cell, a value 12% higher than that of squalane (Table 1).[7] Bhattacharyya's group then used fluorescence correlation spectroscopy at 20 °C to determine diffusion constants for C153[6] in the lipid droplets of a non-cancer lung fibroblast cell (W138) and a human lung cancer cell (A549). When used with eq 1, the D values give viscosities 1.2_5 and 2.1 times that of squalane, respectively.

The previous section's MSE fits and squalene's D values also were used to calculate the difference between the solvents' experimental and calculated viscosities. The AAPDs are given by solvent in Table 4 and solvent group in Table 5. For the viscosities, the AAPD is the average value of (10^2) $(|\eta_{calcd} - \eta_{exptl}|/\eta_{exptl})$.

Table 4. Viscosity Calculations for Squalene's Solvents

			% difference		
solvent	T, °C	$10^2\eta$, P[a]	no CO_2[b]	no HPSM[c]	all 35[d]
n-C_6	23.0	0.306	−13.4	−4.97	−5.19
n-C_8	24.0	0.514	−6.00	−2.08	0.195
n-C_{10}	24.0	0.850	0.841	−0.007	4.81
n-C_{12}	24.0	1.41	−0.611	−5.51	1.11
n-C_{14}	24.0	2.14	1.55	−7.02	1.34
n-C_{16}[e]	22.75	3.18	0.472	−11.0	−1.43
x_i = 0.291[e]	22.5	2.97	−6.75	−16.4	−7.95
x_i = 0.508[e]	22.75	7.24	−4.54	−20.9	−9.47
x_i = 0.708[e]	22.5	13.8	−7.55	−27.3	−14.6
squalane[e]	23.0	30.3	−2.87	−28.9	−13.6
pristane	22.25	7.28	−17.7	−30.9	−21.4
HPMN	24.0	3.52	21.0	4.51	17.2
cyclohexane	24.0	0.910	1.67	0.154	5.32
n-$C_4C_6H_{11}$	24.0	1.23	4.97	0.514	7.18
n-$C_6C_6H_{11}$	24.5	2.02	10.3	0.753	9.94
n-$C_8C_6H_{11}$	23.25	3.24	16.3	1.50	13.2
n-$C_{12}C_6H_{11}$	24.0	6.53	8.25	−10.5	2.57
CD_2Cl_2[f]	10.0	0.482	−2.61	1.71	3.94
CO_2, 18 MPa[g]	41.35	0.0728	−29.4	−10.8	−17.0
CO_2, 17 MPa	41.35	0.0709	−31.1	−12.6	−18.8
CO_2, 16 MPa	41.35	0.0688	−22.5	2.47	−9.04
CO_2, 15 MPa	41.35	0.0665	−26.6	−6.85	−13.5
CO_2, 13 MPa	41.35	0.0602	−27.6	−7.27	−14.3
EtOAc, 1 bar[h]	30.0	0.399	3.57	9.17	11.0
EtOAc, 75 bar	30.0	0.433	3.17	8.03	10.2
EtOAc, 150 bar	30.0	0.464	1.37	5.67	7.99
EtOAc, 1 bar	40.0	0.359	1.90	8.54	9.75
EtOAc, 75 bar	40.0	0.390	0.390	6.31	7.81
EtOAc, 150 bar	40.0	0.419	0.790	6.04	7.88
EtOAc, 1 bar	50.0	0.325	0.702	8.29	8.99
EtOAc, 75 bar	50.0	0.354	−0.028	6.79	7.84
EtOAc, 150 bar	50.0	0.381	−0.280	5.87	7.23
EtOAc, 1 bar	60.0	0.295	−1.49	7.02	7.17
EtOAc, 75 bar	60.0	0.323	−1.89	5.79	6.33
EtOAc, 150 bar	60.0	0.348	−1.34	5.66	6.56

[a]From the refs in the Experimental Methods section. [b]Percentage differences between calculated and experimental viscosities using fit to eq 2 excluding CO_2 data. [c]Same as footnote *c* using fit to eq 2 excluding HPSM data. [d]Same as footnote *c* using fit to eq 2 for all 35 experimental D values. [e]From ref 5 (x_i = mole fraction squalane in n-C_8−squalane mixed solvents). [f]From ref 12. [g]All CO_2 D values are from ref 14. [h]All EtOAc D values are from ref 13.

The fit that excluded the CO_2 data appears to be preferable for the lipid droplet viscosities. It gave the smallest AAPD between the experimental and calculated values for the HPSMs (10.1%, Table 5) and gave a small AAPD of 4.82% for the 30 non-CO_2 solutions. The AAPD for the five CO_2 solutions, the most viscous of which is a factor of ∼4.1 outside the range of the viscosities used in the fit, was 27.4%. The three largest non-CO_2 viscosity differences were for HPMN, +21.0%; pristane, −17.7%; and n-$C_8C_6H_{11}$, +16.3%; squalane's was −2.87%. Figure 4 shows a comparison of the fit's experimental and calculated viscosities. The fit that used all 35 solutions gave a larger AAPD of 14.0% for the HPSM viscosities (Table 5). The

https://doi.org/10.1021/acsomega.2c03842
ACS Omega 2022, 7, 31424−31430

Table 5. AAPD between Experimental and Calculated Viscosities for the Three Fits to eq 2

solvent type	no. of solvents	no CO_2[a]	no HPSMs[a]	all[a]
HPSM	6	10.1	21.5	14.0
CO_2	5	27.4	8.00	14.5
n-C_i	6	3.81	5.10	2.35
cyclohexanes	5	8.30	2.68	7.64
CD_2Cl_2	1	2.61	1.71	3.94
EtOAc	12	1.41	6.93	8.23
AAPD for included		4.82[b]	5.82[c]	8.90[d]

[a]AAPD between experimental and calculated viscosities for each solvent group. [b]AAPD for 30 solvents excluding CO_2 data. [c]AAPD for 29 solvents excluding HPSM data. [d]AAPD for all 35 solvents.

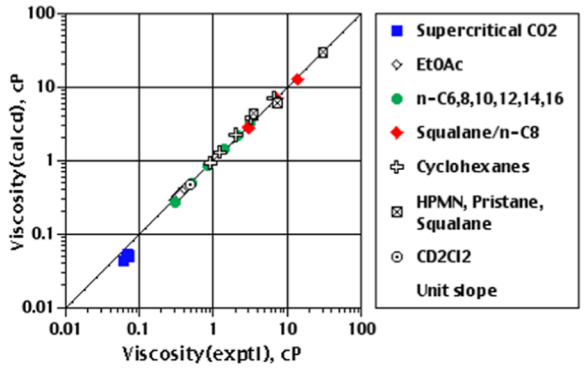

Figure 4. Plot of calculated *vs.* experimental viscosities for squalene's solvents. The calculated values were obtained using the fit that omitted squalene's D values in supercritical CO_2.

largest difference was −21.4% for pristane (Table 4), squalane's was −13.6%, and the AAPD for all 35 solutions was 8.90% (Table 5).

Squalane's viscosity is a factor of 4.6 higher than the most viscous solvent in the fit that excluded the HPSMs (n-$C_{12}C_6H_{11}$, Table 4). Its difference was −28.9% and the AAPD for the HPSMs was 21.5% (Table 5). This AAPD and that for the CO_2 solutions from the fit that excluded them (27.4%) suggest that the uncertainty in viscosities a factor of ∼5 outside our range of η values is ∼25−30%.

Diffusion-ordered NMR spectroscopy[41] is a technique that might be employed to determine squalene's diffusion constant in lipid droplets. It was used to obtain squalene's D value in multi-solute $CDCl_3$ and toluene solutions. The co-solutes in $CDCl_3$ were 1-eicosanol, α-tocopherol, erythrodiol, stigmasterol, β-sitosterol, campesterol, and cycloartenol.[42] Those in toluene were triolein, 1,2-dioleoglycerol, 1,3-dioleoglycerol, 1-oleoyl-rac-glycerol, methyl oleate, and benzene.[43] Squalene's diffusion constants in these two solvents were not used in our analyses because the temperatures were not given. Diffusion-ordered NMR spectroscopy also was used to obtain the D value for squalene in the same CD_2Cl_2 solution (Table 1) with adamantane, and cyclododecane.[12]

Supercritical and Pressure Liquid Extractions. The fit to eq 2 that excluded the higher viscosity HPSMs may be useful for estimating the diffusion constants needed for the supercritical and pressurized liquid extractions by which squalene can be obtained from vegetal sources.[13,44,45] It gives (Table 3) an AAPD of 7.28% between the experimental and calculated D values in the five supercritical CO_2 solutions and 5.53% for the 29 solvents included in the fit. The largest difference is −11.5% in CO_2 at 17 MPa (Table 1). Given that the D values needed for the supercritical and pressurized liquid applications would likely fall within the range of this fit and the 35-solvent fit, a suggested estimate of their uncertainty would be that for the CO_2 data in the 35-solvent fit (12.7%), a value higher than the corresponding values for the fit that omitted the HPSM diffusion constants (7.28%).

Wilke−Chang Correlation. The Wilke−Chang equation (WCE), widely used for estimating D values in liquid chromatography, is given by[15,46]

$$D_{AB} = (7.4 \times 10^{-8})[T(\phi M_B)^{1/2}]/(\eta_B V_A^{0.6}) \quad (3)$$

where D_{AB} ($cm^2\ s^{-1}$) is the diffusion constant of solute A in solvent B, ϕ is the solvent's association factor, η_B (cP) is the solvent's viscosity, M_B ($g\ mol^{-1}$) is the solvent's molar mass, and V_A ($cm^3\ mol^{-1}$) is the solute's molar volume at its normal boiling point, determined using the Le Bas group contribution method.[47]

Calculations were carried out using $V_A = 629\ cm^3\ mol^{-1}$,[47] $\phi = 1$ for our non-associated solvents,[15,46] and $(M_B)_{mixed} = \sum x_i M_{B,i}$ for the molar masses of the three n-C_8−squalane mixtures. x_i and $M_{B,i}$ are the mole fraction and molar mass of solvent i, respectively. As seen in Table 6, the WCE gave an AAPD of

Table 6. AAPD between Experimental and Calculated Diffusion Constants for the WCE and MSE Correlations by the Solvent Group

solvent type	no. of solvents	WCE	MSE[a]
HPSM	6	10.9	12.2
CO_2	5	32.4	12.7
n-C_i	6	5.53	2.03
cyclohexanes	5	7.24	6.59
CD_2Cl_2	1	13.6	3.46
EtOAc	12	6.77	7.07_5
all solvents	35	11.2	7.72
without CO_2	30	7.65	3.96

[a]AAPDs for this column are from the "all" column" in Table 3 except for the "without CO_2" entry which is the "AAPD for included" entry in the "no CO_2" column in Table 3.

11.2% between the experimental and calculated diffusion constants, a value larger than 7.72% for the corresponding MSE fit. As also seen in Tables 6 and 3, the WCE fit gave an AAPD of 10.9% for the HPSMs, slightly better than the 12.2% from the 35-solution MSE fit but worse than the 8.33% for the fit that excluded the CO_2 solutions. When the CO_2 data (AAPD = 32.4%) are excluded, the AAPD for the WCE fit decreases from 11.2 to 7.65% whereas the AAPD for the MSE fit without the CO_2 data was 3.96% (Table 6). The 35 diffusion constants calculated using eq 3 are compared with the experimental values as shown in Figure 5. The WCE cannot be used for lipid droplets' viscosities because the solvent's molar mass is required and their cores have variable compositions. It could be used for estimating squalene's D values for solvents involved in extraction processes but the MSE fit gives better overall agreement with experiment.

Other Possible Uses for Squalene's Diffusion Constants. There have been MD studies of squalene's (a) dynamics in a monolayer on graphite,[16] (b) conformational dynamics in solution,[17] (c) properties at the air/squalene interface,[48] and (d) orientation and phase preference in an H_2O/CCl_4 system.[49] No diffusion constants have been calculated, however, and the

https://doi.org/10.1021/acsomega.2c03842
ACS Omega 2022, 7, 31424−31430

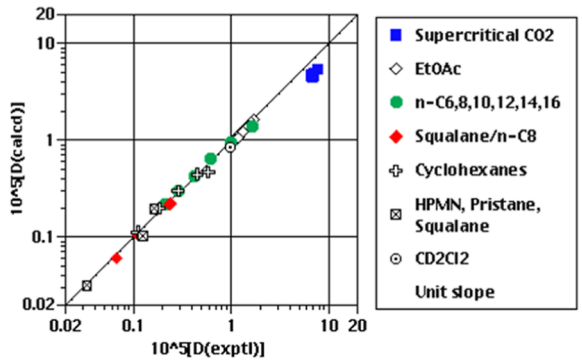

Figure 5. Plot of calculated vs. experimental diffusion constants (in cm^2 s^{-1}) for squalene. The calculated values were obtained using the Wilke−Chang correlation, eq 3, for all 35 of squalene's *D* values.

values given here should provide an adequate test of MD force fields.[50] The codes could then be applied to other processes involving squalene.

The MD simulations in refs 48 and 49 are in agreement with our earlier study[5] that indicated squalene has a relatively extended conformation in nonpolar solutions. The calculations and Figure 4 of ref 48 showed that ∼94% of 343 molecules were relatively extended; ∼45% had all-*anti* methylene bridges, ∼37% had one *gauche* defect, and ∼12% had two. The percentages in bulk squalene and the interface were essentially the same. The calculations in ref 49 gave an elongated conformation in CCl_4. Squalene's conformation and molecular motion in solution are discussed in more detail in ref 5.

Machine learning studies of diffusion have focused on solutes in polar,[19] nonpolar,[19] and supercritical CO_2[18] solvents. The gradient boosted ML algorithm gave the best agreement of 2.58% for 1476 *D* values in CO_2,[18] 5.07% for 430 *D* values in polar solvents,[19] and 5.86% for 342 *D* values in nonpolar solvents.[19] Our *D* values in the alkanes and cyclohexanes are candidates for the solute-nonpolar solvent data set.

A machine learning analysis that determines viscosities from *D* values using single solvent properties has not been carried out but it would present problems for a lipid droplet because its interior is not a single solvent. The MSE fit requires only squalene's diffusion constant and the temperature.

SUMMARY AND CONCLUSIONS

Capillary flow techniques have been used to determine the translational diffusion constant, *D*, of squalene in five *n*-alkanes, two methyl-substituted alkanes, and five cyclohexanes. The *D* values show deviations from the Stokes−Einstein relation, as do published data for squalene in CD_2Cl_2,[12] *n*-C_{16},[5] squalane,[5] *n*-C_8−squalane mixtures,[5] supercritical CO_2,[14] and ethyl acetate.[13]

Three fits of squalene's *D* values to the MSE, $D/T = A_{SE}/\eta^p$, were made. One was motivated by the possibility of using it to make a label-free estimate of the viscosity in the core of lipid droplets. It excluded the data for the least viscous CO_2 solutions because the viscosities in lipid droplets are likely to be near or beyond that of our most viscous solvent, squalane. The fit gave an AAPD of 3.96% between the 30 experimental and calculated diffusion constants in the non-CO_2 solvents.

Another fit included the five *D* values in CO_2 but excluded the diffusion constants in the more viscous HPMN, pristane, squalane, and *n*-C_8−squalane mixtures. It could be useful for estimating squalene's *D* values in the low-viscosity solutions used in extractions from plant sources. The AAPD between the 29 experimental and calculated *D* values was 5.53%. The third fit included all 35 *D* values and gave an AAPD of 7.72%. Fits using the Wilke−Chang correlation with and without the CO_2 diffusion constants were less successful than those using the MSE although the agreement improved when the CO_2 data were not included.

AUTHOR INFORMATION

Corresponding Author

Bruce A. Kowert − *Department of Chemistry, St. Louis University, St. Louis, Missouri 63103, United States;* orcid.org/0000-0002-4030-8670; Phone: 314-977-2837; Email: bruce.kowert@slu.edu; Fax: 314-977-2521

Complete contact information is available at: https://pubs.acs.org/10.1021/acsomega.2c03842

Notes

The author declares no competing financial interest.

ACKNOWLEDGMENTS

The Department of Chemistry, Saint Louis University, supported this research. The data acquisition system and detector were purchased with grants to Dr. Barry Hogan from Research Corp. and the donors of the Petroleum Research Fund, administered by the American Chemical Society.

REFERENCES

(1) Lou-Bonafonte, J. M.; Martínez-Beamonte, R.; Sanclemente, T.; Surra, J. V.; Herrera-Marcos, L. V.; Sanchez-Marco, J.; Arnal, C.; Osada, J. Current Insights into the Biological Action of Squalane. *Mol. Nutr. Food Res.* **2018**, *62*, 1800136.

(2) Zhou, S.; Forbes, M. W.; Abbatt, J. P. D. Kinetics and Products from Heterogeneous Oxidation of Squalene with Ozone. *Environ. Sci. Technol.* **2016**, *50*, 11688−11697.

(3) Spanova, M.; Daum, G. Squalene—Biochemistry, Molecular Biology, Process Biotechnology, and Applications. *Eur. J. Lipid Sci. Technol.* **2011**, *113*, 1299−1320.

(4) Ben M'barek, K.; Ajjaji, D.; Chorlay, A.; Vanni, S.; Forêt, L.; Thiam, A. ER Membrane Phospholipids and Surface Tension Control Cellular Lipid Droplet Formation. *Dev. Cell* **2017**, *41*, 591−604.

(5) Kowert, B. A.; Watson, M. B.; Dang, N. C. Diffusion of Squalene in *n*-Alkanes and Squalane. *J. Phys. Chem. B* **2014**, *118*, 2157−2163.

(6) Chowdhury, R.; Jana, B.; Saha, A.; Ghosh, S.; Bhattacharyya, K. Confocal Microscopy of Cytoplasmic Lipid Droplets in a Live Cancer Cell: Number, Polarity, Diffusion, and Solvation Dynamics. *Med. Chem. Commun.* **2014**, *5*, 536−539.

(7) Ghosh, S.; Chattoraj, S.; Mondal, T.; Bhattacharyya, K. Dynamics in Cytoplasm, Nucleus, and Lipid Droplet of a Live CHO Cell: Time-Resolved Confocal Microscopy. *Langmuir* **2013**, *29*, 7975−7982.

(8) Bosch, M.; Sánchez-Álvarez, M.; Fajardo, A.; Kapetanovic, R.; Steiner, B.; Dutra, F.; Moreira, L.; López, J. A.; Campo, R.; Mari, M.; Morales-Paytuví, F.; Tort, O.; Gubern, A.; Templin, R. M.; Curson, J. E. B.; Martel, N.; Català, C.; Lozano, F.; Tebar, F.; Enrich, C.; Vázquez, J.; Del Pozo, M. A.; Sweet, M. J.; Bozza, P. T.; Gross, S. P.; Parton, R. G.; Pol, A. Mammalian Lipid Droplets Are Innate Immune Hubs Integrating Cell Metabolism and Host Defense. *Science* **2020**, *370*, No. eaay8085.

(9) Green, D. R. Immiscible Immunity. *Science* **2020**, *370*, 294−295.

(10) Shimobayashi, S. F.; Ohsaki, Y. Universal Phase Behaviors of Intracellular Lipid Droplets. *Proc. Natl. Acad. Sci. U.S.A.* **2019**, *116*, 25440.

(11) Starich, M. R.; Tang, J.; Remaley, A. T.; Tjandra, N. Squeezing Lipids: NMR Characterization of Lipoprotein Particles Under Pressure. *Chem. Phys. Lipids* **2020**, *228*, 104874.

(12) Hamdoun, G.; Guduff, L.; van Heijenoort, C.; Bour, C.; Gandon, V.; Dumez, J.-N. Spatially Encoded Diffusion-Ordered NMR Spec-

troscopy of Reaction Mixtures in Organic Solvents. *Analyst* **2018**, *143*, 3458−3464.
(13) Zêzere, B.; Silva, J. M.; Portugal, I.; Gomes, R. B.; Silva, C. M. Measurement of Astaxanthin and Squalene Diffusivities in Compressed Liquid Ethyl Acetate by Taylor-Aris Dispersion Method. *Sep. Purif. Technol.* **2020**, *234*, 116046.
(14) Dahmen, N.; Kordikowski, A.; Schneider, G. M. Determination of Binary Diffusion Coefficients of Organic Compounds in Supercritical Carbon Dioxide by Supercritical Fluid Chromatography. *J. Chromatogr.* **1990**, *505*, 169−178.
(15) Poling, B. E.; Prausnitz, J. M.; O'Connell, J. P. *The Properties of Gases and Liquids 5E*; 5th ed.; McGraw-Hill: New York, 2001; Section 11.9.
(16) Enevoldsen, A. D.; Hansen, F. Y.; Diama, A.; Taub, H.; Dimeo, R. M.; Neumann, D. A.; Copley, J. R. D. Comparative Study of Normal and Branched Alkane Monolayer Films Adsorbed on a Solid Surface. II. Dynamics. *J. Chem. Phys.* **2007**, *126*, 104704.
(17) Pogliani, L.; Milanesio, M.; Ceruti, M.; Viterbo, D. Conformational and Dynamical Study of Squalene Derivatives. III: Azasqualenes and Solvated Squalene. *Chem. Phys. Lipids* **1999**, *103*, 81−93.
(18) Aniceto, J. P. S.; Zêzere, B.; Silva, C. M. Machine Learning Models for the Prediction of Diffusivities in Supercritical CO_2 Systems. *J. Mol. Liq.* **2021**, *326*, 115281.
(19) Aniceto, J. P. S.; Zêzere, B.; Silva, C. M. Predictive Models for Binary Diffusion Coefficients at Infinite Dilution in Polar and Nonpolar Fluids. *Materials* **2021**, *14*, 542.
(20) Lu, H.-T.; Jiang, Y.; Chen, F. Determination of Squalene Using High-Performance Liquid Chromatography with Diode Array Detection. *Chromatographia* **2004**, *59*, 367−371.
(21) Kowert, B. A.; Watson, M. B. Diffusion of Organic Solutes in Squalane. *J. Phys. Chem. B* **2011**, *115*, 9687−9694.
(22) Taylor, G. I. The Dispersion of Matter in Turbulent Flow through a Pipe. *Proc. R. Soc. London, Ser. A* **1954**, *223*, 446−468.
(23) Birovljev, B.; Måløy, K. J.; Feder, J.; Jøssang, T. Scaling Structure of Tracer Dispersion Fronts in Porous Media. *Phys. Rev. E: Stat. Phys., Plasmas, Fluids, Relat. Interdiscip. Top.* **1994**, *49*, 5431−5437.
(24) Boschan, A.; Auradou, H.; Ippolito, I.; Chertcoff, R.; Hulin, J. P. Miscible Displacement Fronts of Shear Thinning Fluids Inside Rough Fractures. *Water Resour. Res.* **2007**, *43*, W03438.
(25) Taylor, G. I. Conditions under Which Dispersion of a Solute in a Stream of Solvent can be Used to Measure Molecular Diffusion. *Proc. R. Soc. London, Ser. A* **1954**, *225*, 473−477.
(26) Viswanath, D. S.; Natarajan, G. *Data Book on the Viscosity of Liquids*; Hemisphere Publishing: New York, 1989.
(27) Prak, D. J. C.; Trulove, P. C.; Cowart, J. S. Density, Viscosity, Speed of Sound, Surface Tension, and Flash Point of *n*-Hexadecane and 2,2,4,4,6,8,8-Heptamethylnonane and of Algal-Based Hydrotreated Renewable Diesel. *J. Chem. Eng. Data* **2013**, *58*, 920−926.
(28) El-Tahir, A.; Boned, C.; Lagourette, B.; Xans, P. Determination of the Viscosity of Various Hydrocarbons and Mixtures of Hydrocarbons Versus Temperature and Pressure. *Int. J. Thermophys.* **1995**, *16*, 1309−1334.
(29) Barlow, A. J.; Erginsav, A.; Lamb, J. Viscoelastic Relaxation of Supercooled Liquids. II. *Proc. R. Soc. London, Ser. A* **1967**, *298*, 481−494.
(30) Papanastasiou, G. E.; Ziogas, I. I. Physical Behavior of Some Reaction Media. Density, Viscosity, Dielectric Constant, and Refractive Index Changes of Ethanol-Cyclohexane Mixtures at Several Temperatures. *J. Chem. Eng. Data* **1991**, *36*, 46−51.
(31) Rossini, F. D.; Pitzer, K. S.; Arnett, R. L.; Braun, R. M.; Pimentel, G. C. *Selected Values of Physical and Thermodynamic Properties of Hydrocarbons and Related Compounds*; Carnegie Press: Pittsburgh, 1953.
(32) Fenghour, A.; Wakeham, W. A.; Vesovic, V. The Viscosity of Carbon Dioxide. *J. Phys. Chem. Ref. Data* **1998**, *27*, 31−44.
(33) Yaws, C. L.. *Handbook of Viscosity*; Gulf Publishing Co.: Houston, 1995; Vol. *1*.
(34) Tyrrell, H. J. V.; Harris, K. R. *Diffusion in Liquids*; Butterworths: London, 1984.
(35) Longuet-Higgins, H. C. Transport Processes in Fluids. *Il Nuovo Cimento* **1955**, *1*, 140−155.
(36) Kowert, B. A.; Sobush, K. T.; Fuqua, C. F.; Mapes, C. L.; Jones, J. B.; Zahm, J. A. Size-Dependent Diffusion in the *n*-Alkanes. *J. Phys. Chem. A* **2003**, *107*, 4790−4795.
(37) Zwanzig, R.; Harrison, A. K. Modifications of the Stokes-Einstein Formula. *J. Chem. Phys.* **1985**, *83*, 5861−5862.
(38) Chen, S. H.; Davis, H. T.; Evans, D. F. Tracer Diffusion in Polyatomic Liquids. III. *J. Chem. Phys.* **1982**, *77*, 2540−2544.
(39) Harris, K. R. The Fractional Stokes-Einstein Equation: Application to Lennard-Jones, Molecular, and Ionic Liquids. *J. Chem. Phys.* **2009**, *131*, 054503.
(40) Chan, T. C.; Tang, W. K. Diffusion of Aromatic Compounds in Nonaqueous Solvents: A Study of Solute, Solvent, and Temperature Dependence. *J. Chem. Phys.* **2013**, *138*, 224503.
(41) Hinton, D. P.; Johnson, C. S., Jr. Diffusion Ordered 2D NMR Spectroscopy of Phospholipid Vesicles: Determination of Vesicle Size Distributions. *J. Phys. Chem.* **1993**, *97*, 9064−9072.
(42) Altun, A.; Ok, S. NMR Analyses and Diffusion Coefficient Determination of Minor Constituents of Olive Oil: Combined Experimental and Theoretical Studies. *J. Chem. Eng. Data* **2012**, *57*, 2619−2624.
(43) Socha, A. M.; Kagan, G.; Li, W.; Hopson, R.; Sello, J. K.; Williard, P. G. Diffusion Coefficient-Formula Weight Correlation Analysis via Diffusion-Ordered Nuclear Magnetic Resonance Spectroscopy (DOSY NMR) to Examine Acylglycerol Mixtures and Biodiesel Production. *Energy Fuels* **2010**, *24*, 4518−4521.
(44) Oliveira, E. L. G.; Silvestre, A. J. D.; Silva, C. M. Review of Kinetic Models for Supercritical Fluid Extraction. *Chem. Eng. Res. Des.* **2011**, *89*, 1104−1117.
(45) Barbosa, A. M.; Santos, K. S.; Borges, G. R.; Muniz, A. V. C. S.; Mendonça, F. M. R.; Pinheiro, M. S.; Franceschi, E.; Dariva, C.; Padilha, F. F. Separation of Antibacterial Biocompounds from *Hancornia speciosa* Leaves by a Sequential Process of Pressured Liquid Extraction. *Sep. Purif. Technol.* **2019**, *222*, 390−395.
(46) Wilkie, C. R.; Chang, P. Correlation of Diffusion Coefficients in Dilute Solutions. *AIChE J.* **1955**, *1*, 264−270.
(47) Reference 13, Section 4.10.
(48) von Domaros, M.; Liu, Y.; Butman, J. L.; Perlt, E.; Geiger, F. M.; Tobias, D. J. Molecular Orientation at the Squalene/Air Interface from Sum Frequency Generation Spectroscopy and Atomistic Modeling. *J. Phys. Chem. B* **2021**, *125*, 3932−3941.
(49) Guba, W.; Kessler, H. A Novel Computational Mimetic of Biological Membranes in Molecular Dynamics Simulations. *J. Phys. Chem.* **1994**, *98*, 23−27.
(50) Papavasileiou, K. D.; Peristeras, L. D.; Bick, A.; Economou, I. G. Molecular Dynamics Simulation of Pure *n*-Alkanes and Their Mixtures at Elevated Temperatures Using Atomistic and Coarse-Grained Force Fields. *J. Phys. Chem. B* **2019**, *123*, 6229−6243.

https://doi.org/10.1021/acsomega.2c03842
ACS Omega 2022, 7, 31424−31430